Renewable Energy 207 (2023) 601–610

Contents lists available at ScienceDirect

Renewable Energy

journal homepage: www.elsevier.com/locate/renene

Effect of semi-transparent a-Si PV glazing within double-skin façades on visual and energy performances under the UK climate condition

Frank Roberts [a], Siliang Yang [a,*], Hu Du [b,c], Rebecca Yang [d]

[a] School of Built Environment, Engineering and Computing, Leeds Beckett University, Leeds, United Kingdom
[b] School of Civil Engineering and Built Environment, Liverpool John Moores University, Liverpool, United Kingdom
[c] Welsh School of Architecture, Cardiff University, Cardiff, United Kingdom
[d] School of Property, Construction and Project Management, RMIT University, Melbourne, Australia

ARTICLE INFO

Keywords:
Building-integrated photovoltaic systems
Double-skin façade
Indoor lighting
Building energy consumption
DesignBuilder
Building simulation

ABSTRACT

Various studies have assessed the energy performance alterations affected by the novel technology of Building-Integrated Photovoltaic in Double-Skin Facades (BIPV-DSF), while lighting performance tied to the BIPV-DSF has not received much attention. This paper provides numerical modelling to assess the effect of BIPV-DSF on both indoor visual condition and energy consumption for an office module under a typical climate in the United Kingdom. The proposed study was focused on the comparisons between a reference case (a DSF office module with both layers using clear double glazing) and a design case of the same office module with BIPV-DSF using semi-transparent Amorphous Silicon PV glazing. Results show a significant drop in maximum daylight illuminance of 73% by configuring the BIPV-DSF with reference to the regular DSF. It was also reported the resultant average and minimum daylight factors (0.65% and 0.00%) were not able to meet indoor visual comfort requirements for office environments. Furthermore, it was found that the use of BIPV-DSF resulted in a net increase of 8% in building energy consumption over the reference DSF. Therefore, it is concluded that in the present context the BIPV-DSF is not viable for a commercial installation under the UK's climate conditions.

1. Introduction

With building design continuously evolving, developments and innovative technologies have been driving the traditional buildings' functionality far beyond just bricks and mortar [1]. Statistically, buildings are claimed to consume approximately 40% of global energy consumption [2]. Therefore, governments across the world are implementing Net Zero Carbon Strategies, which include the increase of renewable energy generation and reduction of building energy consumption, where engineers and architects are introducing passive design strategies to enhance efficiency whilst maintaining user comfort and reducing the problematic effects of global warming and greenhouse gas production [3].

To achieve the Net Zero target, collective efforts in carbon reduction and renewable energy generation are needed to decarbonise the existing building stock [4–6]. The Building Integrated Photovoltaic in Double-Skin Facade (BIPV-DSF) is one of promising façade technologies that offers the potential to reduce carbon emission through passive solution and generate renewable energy [7]. In terms of the application, BIPV-DSF has effects on multiple factors, such as indoor lighting environment, indoor thermal comfort, energy consumption of artificial lighting, heating, and cooling [8]. However, limited studies have been conducted to understand the multi-faceted impact of BIPV-DSF on indoor environment, particularly for the UK climate [9].

The paper will conclude alterations in lighting conditions and indicates energy performance differences between a DSF with both clear and semi-transparent BIPV glazing methods. Especially, the proposed study in this paper investigates the effect of the BIPV-DSF on natural daylighting and energy performance within a case study of office building based in London of the UK. The paper comprises five sections, of which Section 1 (Introduction) states the context of the proposed research study and indicates the research gaps, which are further discussed in Section 2 (Literature review and research gaps) based upon a literature review about the BIPV-DSF. The research methods adopted in this study are specified in Section 3 (Methodology), while the results of the study are presented and discussed in Section 4 (Results and discussion). Finally, the paper is summarised in Section 5 (Conclusions), which also points out the limitations of the proposed research and recommendations for future work.

* Corresponding author. School of Built Environment, Engineering and Computing, Leeds Beckett University, Leeds, LS2 8AG, United Kingdom.
E-mail address: s.yang@leedsbeckett.ac.uk (S. Yang).

https://doi.org/10.1016/j.renene.2023.03.023
Received 23 April 2022; Received in revised form 2 November 2022; Accepted 5 March 2023
Available online 7 March 2023

Nomenclature

Symbols

A_i	inside surface area [m^2]
A_{surf}	semi-transparent PV glazing surface area [m^2]
a, b, c, d, e	adjustable coefficients in relation to insolation conditions [−]
C_p	zone air specific heat capacity [J/kg·K]
f_{active}	fraction of surface area with active solar cells [−]
G_T	total solar radiation incident on PV glazing [W/m^2]
h_i	heat transfer coefficient [W/m^2·K]
I_{sc}	short circuit current of PV module [A]
$\dot{m}_i$	interzone air mass flow rate [kg/h]
$\dot{m}_{inf}$	outside air mass flow rate due to infiltration [kg/h]
$\dot{m}_{sys}$	supply air mass flow rate [kg/h]
P_{mpp}	maximum power of PV module [W_p]
$\dot{Q}_i$	internal load [kW]
$\dot{Q}_{load}$	net zone thermal load [kW]
$\dot{Q}_{sys}$	air system thermal load [kW]
T_{si}	inside surface temperature [K]
T_{sup}	supply air temperature [K]
T_z	zone mean air temperature [K]
T_{zi}	interzone air temperature [K]
T_∞	outside air temperature [K]
U-value	thermal transmittance [W/m^2·K]
V_{oc}	open circuit voltage of PV module [V]

Greek symbols

γ	angle between sky and sun's position [°]
ζ	zenith angle of sky element considered [°]
η_{PV}	PV efficiency [%]
θ	azimuth angle of a sky or ground element [°]
$L_e(\theta_r,\Phi_r)$	emitted radiance [cd/m^2]
$L_i(\theta_i,\Phi_i)$	incident radiance [cd/m^2]
$L_r(\theta_r,\Phi_r)$	reflected radiance [cd/m^2]
l_v	relative luminance [cd/m^2]
$\rho_{bd}(\theta_i,\Phi_i;\theta_r,\Phi_r)$	bi-directional reflectance-transmittance distribution function per steradian
Φ	altitude angle of a sky or ground element [°]

Abbreviations

ACH	air changes per hour
a-Si	amorphous silicon
BIPV	building-integrated photovoltaic
BIPV-DSF	building-integrated photovoltaic in double-skin facade
CdTe	cadmium telluride
CIGS	copper indium gallium selenide
DA	daylight autonomy
DC	daylight coefficient
DF	daylight factor
DGP	daylight glare probability
DSF	double-skin facade
DSSC	dye-sensitised solar cell
HVAC	heating, ventilation, and air conditioning
PV	photovoltaic
SCoP	seasonal coefficient of performance
SHGC	solar heat gain coefficient
STC	standard test condition
UDI	useful daylight illuminance
VLT	visible light transmittance

2. Literature review and research gaps

Over the last few decades, the design of traditional façade technology has developed to consider sustainability, low energy consumption and indoor comfort at its core [10]. One of these façade innovations, known as double-skin facade (DSF), is a multi-layer skin approach to the construction of the external face of a building, implementing an external skin, a cavity space, and an inner skin at its core [11]. DSF is also considered an adaptive façade [12], which can optimise the interaction with the surrounding environment [13].

The fundamental performance characteristics of the DSF are primarily influenced by the ventilation method deployed within the cavity space, as well as the typical construction material selection [14]. In warmer climates or warm summer periods, studies such as Hashemi et al. [15] and Zomorodian et al. [16], find reductions in cooling load by altering airflow within the cavity of the DSF. Whereas Wang et al. [17] found that DSF, in cooler climates or over winter periods, can minimise heat losses when the cavities are sealed, improve heat losses and reduce heating load.

Chan et al. [18] assessed the energy performance of a DSF installation on a typical office building in Hong Kong. Using the EnergyPlus simulation engine, a model was produced to assess different DSF design parameters, such as glazing type (that is, reflectance, absorbance and transmittance), glazing position and glazing layers (that is, single or double-glazed unit). Specifically, in this study in Hong Kong, single inner-single outer, single inner-double outer, double inner-single outer and double inner-double outer were modelled. For a base case, the study [18] used a single skin glass façade with adsorptive glass, then calculated and compared the above configurations with varying glazing types at different orientation. It was concluded that the single outer-double and inner double-skin configuration with reflective glazing could provide 26.7%, 27.7%, 27.3% and 19.2% of cooling energy efficiencies in the East, South, West and North orientations, respectively. They concluded an impractical payback period of 81 years; however, there was no determination of a method to increase efficiency through different ventilation methods within the cavity space, nor was a reference to any effects on visual comfort in terms of illuminance or glare level.

In terms of thermal behaviour, Zhu and He [19] studied heat transfer through DSF, and found that the closed cavity of the non-ventilated DSF achieved 27% and 24% of reductions in heat transfer coefficient for the entire DSF respectively in summer and winter, and therefore the improvement of thermal performance – enhancement in thermal insulation – for buildings. On the other hand, it was found that a ventilated DSF had better thermal insulation than a single skin façade with double glazing, by choosing the optimal cavity depth. However, the optimal cavity depth was not reported in this study, and the interior lighting condition was not mentioned as well.

To further improve the efficiency of DSF, a few group studies over the last decade, have been taken place to investigate how the uptake of the novel semi-transparent photovoltaic glazing in DSF can improve the overall energy and thermal performance for buildings.

Persistent research of the building-integrated photovoltaic system in DSF (BIPV-DSF) being carried on by a research group from Hong Kong across the last decade. Han et al. [20] analysed a BIPV glazed DSF, in comparison with a single skin façade system with normal window glazing and found that the BIPV-DSF could reduce about 5 °C indoor air temperature at summer peak time in Hong Kong. Then, Peng et al. [21] conducted an experiment of a semi-transparent BIPV-DSF building by comparing non-ventilation and buoyancy-driven ventilation within the air cavity. It was found that the buoyancy ventilated BIPV-DSF delivered a better performance than the non-ventilated BIPV-DSF in generating

electricity as well as reducing heat gain and loss through the building façades. It was also reported that the lowest solar heat gain coefficient (SHGC) of the proposed façade was found in the ventilated DSF, which could improve the PV efficiency in Hong Kong (a subtropical climate) through the lowered solar transmission, while the non-ventilated BIPV-DSF had better performance in reducing heat loss of the building during cold period. However, the façade performance in seasons other than winter was not investigated, while the visual comfort was not investigated in either season.

Subsequently, Peng et al. [22] made a simulative study (using EnergyPlus as the simulation tool) for a test office building. It configured the buoyancy ventilated BIPV-DSF system, which was operated in a cool-summer Mediterranean climate zone with regard to the depth of the air cavity, annual power generation, and daylighting performance of the ventilated BIPV-DSF system. It was found that 400 mm–600 mm could be an optimal range of the cavity depth of the BIPV-DSF in terms of energy use, costs and façade cleaning and maintenance. It was also reported that the ventilated BIPV-DSF saved about 35% of electricity consumption, compared with the non-ventilated ones. In addition, it was demonstrated that the BIPV-DSF could generate 65 kWh/m^2/year electricity approximately, which was enough to support the lighting power necessary for most of the time for the test office building. However, the study showed only the daylighting illuminance of the working plane on a monthly average basis, which was limited in understanding the actual situations of visual comfort.

Qiu and Yang [23] in recent years performed a study evaluating energy efficiency of semi-transparent photovoltaic vacuum glazing on buildings within the Greater China area including the cities of Harbin, Kunming, Beijing, Wuhan and Hong Kong. The study considered a baseline of conventional building envelopes in these cities, and using EnergyPlus as the simulation tool, concluded that in terms of annual energy consumption for cooling and heating, vacuum PV glazing reduced overall energy consumption by 28.7%–34.0%, 23.0%–42.1%, 38.6%–44.6%, 31.8%–39.3% and 20.7%–29.2% respectively to the locations aforementioned. However, in moderate climates like Kunming, additional cooling energy is required. Qiu and Yang [23] also assessed visual comfort and daylight implications using DAYSIM programme. Assessing the Useful Daylight Illuminance (UDI) and Daylight Glare Probability (DGP), they compared transparent vacuum glazing with PV vacuum glazing, and found that PV vacuum glazing provided a balanced daylight availability and visual comfort within the room compared to the transparent vacuum glazing. Basically, the PV vacuum glazing was found to provide the best daylight control in low latitude regions such as Wuhan, Hong Kong and Kunming. It is noted however, that these results were based merely on single skin façade buildings.

In the context of Australian climatic conditions, a series of studies [24–27] continued to research the energy consumption and indoor thermal condition in association with integrating the technologies of DSF and semi-transparent photovoltaic glazing. Similar to the previous studies, a test building was presented where three types of cavity ventilation (no, natural and mechanical ventilations), three types of PV glazing (Dye-sensitised solar cell (DSSC), Perovskite-based and Amorphous Silicon (a-Si)) and three locations (Darwin, Sydney and Canberra) were investigated. The study showed that no matter what the location and PV installation type were selected, the lowest cooling demand was achieved through mechanically controlled cavity ventilation. Whereas the lowest heating demand was present with a non-ventilated air cavity. The Perovskite-based PV glazing was able to produce the highest amount of electricity due to its efficiency, with little influence from the cavity ventilation method. Amongst other conclusions associated with specific ventilation configurations, it is noted that very little investigation into the effects of daylighting was considered during this series of research studies; although the low visible light transmittance (VLT) Perovskite-based PV glazing was identified the best in maintaining indoor thermal comfort in warm climates, while the same PV glazing with high VLT was desired for thermal comfort purposes in cold climates.

In summary, the existing literature primarily focused on the energy performance properties dominated by DSF systems within commercial buildings, where more recent papers also assessed the integration of BIPV glazing and the effect on energy performance as well as indoor thermal comfort in different locations globally, but not the UK. However, few studies assessed the effect on visual comfort indoors when both DSF and BIPV glazing systems are integrated (BIPV-DSF). As a matter of fact, visual comfort is a fundamental aspect of building design, contributing to safety, productivity and welfare [28]. Therefore, buildings incorporating BIPV-DSF need to be assessed to understand what effect on daylighting can be anticipated for visual comfort, and what methods are required to mitigate any issues arose. In this context, this paper conducts a comprehensive assessment regarding the impact on both visual comfort and thermal loads when traditional DSF with clear glazing methods are switched to BIPV glazing methods based upon the climatic condition of the United Kingdom.

3. Methodology

3.1. Overview of case study building modelling

In this study, a standard south facing office module in London, United Kingdom, was assessed based on the geometry previously characterised in the work of Yang et al. [26] and Peng et al. [21]. The proposed office module has a length of 2.3 m, a width of 2.44 m and a height of 2.47 m, with an overall gross floor area of 5.6 m^2. Fig. 1 shows the proposed independent office module presenting the double-skin façade structure, where an air cavity is seen between the externally and internally vertical insulation barriers. This cavity was subject to a natural ventilation method driven by the ventilation louvres at the lower and higher positions of the external wall of the double-skin facade. Each of the ventilation louvres had an identical opening area of 1.15 m^2. The cavity ventilation played a significant role in cooling the photovoltaic and preventing overheating issues for the building by natural convention. The “Cavity Zone” was modelled at 0.4 m of depth as this was proven to be within the range of optimum cavity depth in terms of cost, energy use and maintenance [22]. It was assumed that the cavity ventilation method had no effect on the daylight levels. Further, it was also assumed the external window was subject to the sun path characteristics throughout the year, and no other structures provide shading effect throughout the day which would influence daylight.

The external southernly facing façade has a surface area of 6.03 m^2, with a glazing area of 3.74 m^2 giving a total glazing ratio of 62% for both internal and external layers of the façade. The BIPV glazing was

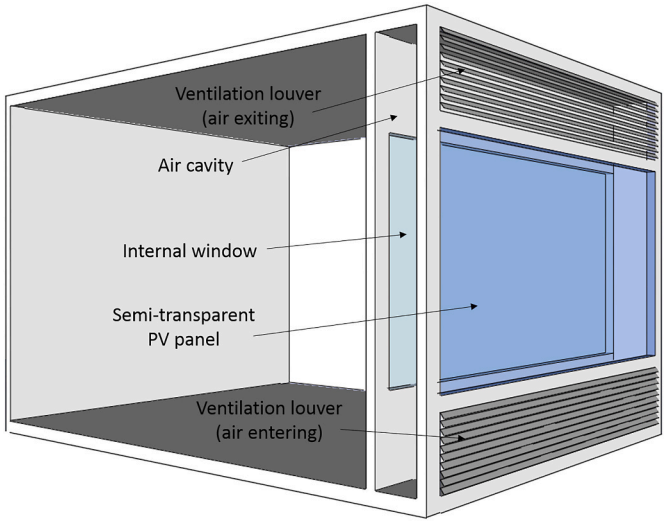

Fig. 1. The office room model with DSF and semi-transparent PV glazing [26].

positioned centrally within the external layer of the façade, within a thermal break aluminium frame. The office module was modelled to meet the minimum thermal and optical requirements defined within UK Building Regulations Part L2A, and the values are summarised in Table 1. It was assumed that there were 9 m^2 per person at working hours during weekdays. The HVAC and lighting systems configuration for the office module were specified in Table 2, while artificial lighting was used to compensate for the possible lack of natural light in the room, to meet the illuminance level requirement of 300 lux for office areas defined by The Society of Light and Lighting [29].

In terms of the characteristics of BIPV glazing, Ghosh et al. [31] produced research around the BIPV types, structure and performance. They defined the BIPV glazing types as first-generation amorphous silicon (a-Si), second generation a-Si, cadmium telluride (CdTe), copper indium gallium selenide (CIGS), and third generation dye-sensitised solar cells (DSSC) and Perovskite. It is noted, however, that both DSSC and Perovskite have inherited stability issues which effect their installation practicality in outdoor environments. The laboratory tests conclude that a-Si, CdTe and CIGS have achieved efficiency ratings of 11.9%, 21.7% and 21.4% respectively, although a-Si based BIPVs provide reasonable daylight transmittance, making it a popular solution for commercial installations despite the reduced efficiency. Therefore, the daylighting analysis in the proposed study was based on a commercially available product of a manufacturer (Onyx Solar Group LLC) – a-Si type of BIPV glazing (as described in Table 3) on the office module. However, the use of low visible light transmittance (VLT) of the a-Si PV glazing rather fell within the object of the proposed study.

Given that the data specified in Table 3, the semi-transparent BIPV window glazing for the office module have been modelled using DesignBuilder V7 based on the manufacturer's specification (Onyx Solar, product number: GL.06), which meet requirement of thermal characteristics for window glazing specified in the Building Regulations Part L2A (as presented in Table 1). Furthermore, Fig. 2 demonstrates the two DSF models used in the study (window facing south), which reflect the generic thermal and visual settings.

Specifically, Model 1 represents a baseline DSF office module providing a double-glazed unit on both the external façade and internal partition. The Model 1's thermal characteristics were described in Table 1. In comparison, Model 2 represents the integration of the BIPV glazing and DSF in the office module, where the external façade glazing was replaced with the semi-transparent a-Si PV glazing based on the specification given in Table 3, while the internal partition glazing matched the specification defined for the Model 1. All the other aspects of the Model 2 matched that of Model 1.

This study was conducted through simulation modelling using embedded calculation engines of Radiance, DAYSIM and EnergyPlus within DesignBuilder V7 programme. Annual climate-based daylighting calculations using the Radiance and DAYSIM performed in this paper were in line with the assessment method defined in BREEAM UK New Construction for Non-domestic Buildings [32]. This assessment method was used as the benchmark to assess the daylighting conditions of the two DSF models. The SLL Code for Lighting [29] was used to determine the recommended illuminance levels and daylighting uniformity ratio (the ratio between the minimum and average daylight factors on the working plane within a room) for office environments by the BREEAM assessment method. Given the proposed study was focused mainly on visual comfort, so the calculation of energy consumptions was only used to take part in the overall performance comparison between both models – Models 1 and 2, which was performed using EnergyPlus simulation engine in DesignBuilder V7.

In terms of model validation, this study focused mainly on the comparison for the different DSF cases but in the same context (the use of external façade window glazing was the only variable), in which the simulation results were used to identify the discrepancy between the two DSF models rather than a single case developed in DesignBuilder. As a matter of fact, the DesignBuilder based BIPV-DSF modelling has been validated through various studies [33–35], which, therefore, was applied to this study.

Table 1
Thermal and optical properties of the building fabric for the office module.

Parameters	Value	Requirement from the Building Regulations Part L2A [30]
U-value of external wall	0.24 W/m^2·K	≤0.35 W/m^2·K
U-value of external roof	0.25 W/m^2·K	≤0.25 W/m^2·K
U-value of floor	0.25 W/m^2·K	≤0.25 W/m^2·K
U-value of windows	1.64 W/m^2·K	≤2.2 W/m^2·K
Solar transmittance of windows	40%	≤40%
Visible light transmittance (VLT) of internal window	69.1%	≤71%

Table 2
HVAC and lighting systems configuration for the office module.

Systems	Configurations
Lighting	LED with 4-step dimming control (2.5 W/m^2 – 100 lux) 2 illuminance sensors at 0.7 m working plane height covering 50% of the room for each
Heating	Natural gas boiler with SCoP of 0.83, Fan Coil Unit
Cooling	Air conditioning with SCoP of 1.67, Air Cooled Chiller, Fan Coil Unit
Mechanical ventilation	Scheduled minimum fresh air per person and per floor area
Office appliances	11.77 W/m^2 at working hours during weekdays
Infiltration	0.3 ACH

Table 3
Properties of the selected semi-transparent a-Si PV glazing.

Parameters	Value	Source
U-value	1.64 W/m^2·K	Manufacturer specification
Solar transmittance	15%	Manufacturer specification
Visible light transmittance (VLT)	20%	Manufacturer specification
Number of modules	3	Design specification
Solar cell type	Amorphous Silicon (a-Si) thin film	Manufacturer specification
Maximum power (P_{mpp}) per module	43 W_p	Manufacturer specification
Open Circuit Voltage (V_{oc})	34 V	Manufacturer specification
Short Circuit Current (I_{sc})	2.25 A	Manufacturer specification
Temperature coefficient of V_{oc}	−0.28%/°C	Manufacturer specification
Temperature coefficient of I_{sc}	+0.09%/°C	Manufacturer specification
Temperature coefficient of P_{mpp}	−0.19%/°C	Manufacturer specification
PV efficiency (under STC)	3.42%	Calculated using maximum power (P_{mpp}) and PV module size

3.2. The mathematical model

All the calculations in this study were performed by using DesignBuilder V7. The DAYSIM simulation engine was used for daylight modelling, which can produce useful daylight illuminance (UDI) distribution plots and calculation summary reports. In addition, the Radiance ray-tracing simulation engine was used to estimate daylight illuminance distribution under static sky conditions and calculate the daylight uniformity and daylight factor. In terms of the energy performance of the proposed office module, the integrated EnergyPlus engine in DesignBuilder was used for predicting the usages of electrical lighting

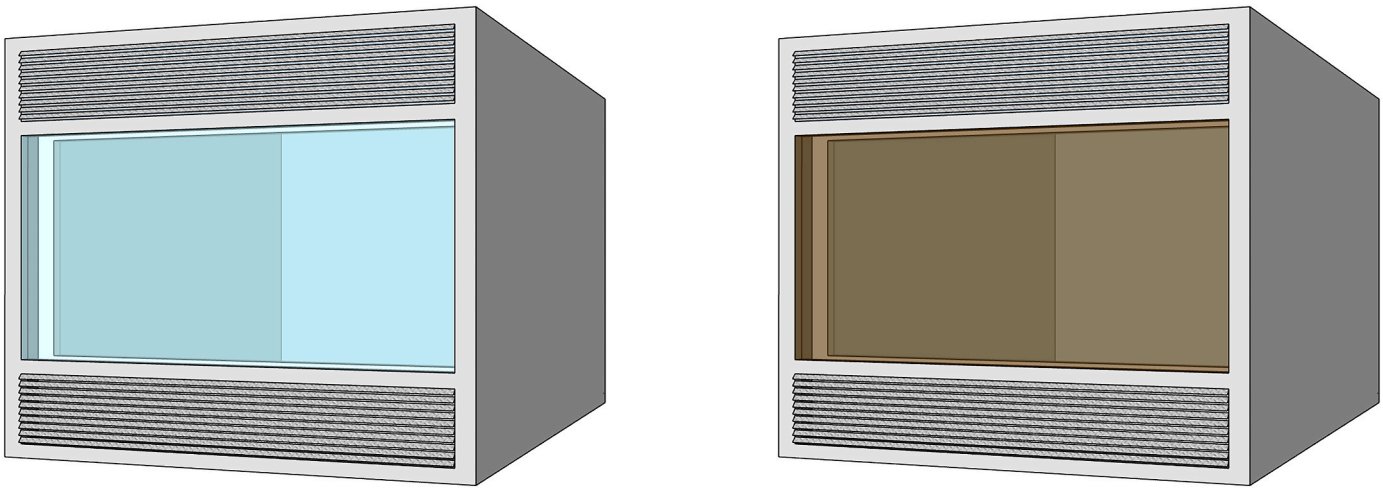

Fig. 2. The proposed models of the DSF office module – Model 1 (left) and Model 2 (right).

energy. London Gatwick EPW weather file from EnergyPlus.net website (GBR_London.Gatwick.037760_IWEC.epw) was used for annual energy simulation.

The Radiance calculation is based on Eq. (1), which is known as "Rendering Equation". This formula has been used within the lighting industry for decades, defining the energy transfer between two points and through a singular point in a particular direction [36].

$$L_r(\theta_r,\Phi_r) = L_e(\theta_r,\Phi_r) + \int_0^{2\pi}\int_0^{\pi} L_i(\theta_i,\Phi_i)\rho_{bd}(\theta_i,\Phi_i;\theta_r,\Phi_r)|cos\ \theta_i|sin\ \theta_i d\theta_i d\Phi_i \tag{1}$$

Where θ is the azimuth angle of a sky or ground element, Φ is the altitude angle of a sky or ground element. $L_e(\theta_r,\Phi_r)$, $L_r(\theta_r,\Phi_r)$ and $L_i(\theta_i,\Phi_i)$ are the emitted, reflected and incident radiance, respectively. $\rho_{bd}(\theta_i,\Phi_i;\theta_r,\Phi_r)$ is the bi-directional reflectance-transmittance distribution function per steradian.

Fundamentally, DAYSIM uses the daylight coefficient (DC) as a method to produce annual daylighting simulations at a fast pace, founded on the sky climate-based model. When assessing advanced glazing types, performance metrics such as daylight autonomy (DA), annual daylight glare probability (DGP) and useful daylight illuminance (UDI) are calculated through the DAYSIM engine, where various subsequent studies [37–39] have validated the accuracy of the simulations founded on the following equation (Eq. (2)) presented by Perez, Seals [40].

$$l_v = f(\zeta,\gamma) = \left[1 + a \bullet exp\left(\frac{b}{cos\ \zeta}\right)\right] \times \left[1 + c \bullet exp(d \bullet \gamma) + e \bullet cos^2\ \gamma\right] \tag{2}$$

Where l_v is the relative luminance, ζ is the zenith angle of the sky element considered, γ is the angle between the sky angle and the sun's position. The letters *a, b, c, d, e* are adjustable coefficients which reflect the insolation conditions.

As mentioned earlier, this study was also designed to predict the overall performance of the BIPV-DSF on thermal (in relation to energy consumption) and visual conditions for the office module. Therefore, the following thermal equations represent the foundational calculation methods used in DesignBuilder under the EnergyPlus simulation engine was used to estimate the energy consumptions and PV electrical production. According to the research output of Taylor et al. [41], heat balance and zone air are the starting points when calculating total air system integration through the thermal zones in buildings. The following equation (Eq. (3)) was programmed within EnergyPlus to determine heating and cooling loads within the office module of this study:

$$\dot{Q}_{load} = \sum_{i=1}^{N_{st}} \dot{Q}_i + \sum_{i=1}^{N_{surf}} h_i A_i (T_{si} - T_z) + \sum_{i=1}^{N_{zones}} \dot{m}_i C_p (T_{zi} - T_z) + \dot{m}_{inf} C_p (T_\infty - T_z) \tag{3}$$

Where $\dot{Q}_i$ is the internal load, $h_i A_i (T_{si} - T_z)$ is the convective heat transfer from the zone surfaces, $\dot{m}_i C_p (T_{zi} - T_z)$ is the heat transfer due to inter-zone air mixing, and $\dot{m}_{inf} C_p (T_\infty - T_z)$ is the heat transfer due to infiltration of outside air.

The air system ensures that hot or cold air is provided within each zone to meet its heating and/or cooling loads. The energy provided by the system into the zone can therefore be formulated as the difference between the supply and exhaust air enthalpies leaving the zones as per Eq. (4).

$$\dot{Q}_{sys} = \dot{m}_{sys} C_p \left(T_{sup} - T_z\right) \tag{4}$$

Where $\dot{m}_{sys}$ is the mass flow rate provided by the air system, C_p is the zone air specific heat, T_{sup} is the supply air temperature, T_z is the zone mean air temperature.

The usable electrical power production produced by the BIPV-DSF are calculated in the form of a simple photovoltaic model in the EnergyPlus simulation engine using Eq. (5).

$$P = A_{surf} \bullet f_{active} \bullet G_T \bullet \eta_{PV} \tag{5}$$

Where A_{surf} is the surface area of the semi-transparent PV glazing, f_{active} is the fraction of surface area with active solar cells, G_T is the total solar radiation incident on the PV glazing, η_{PV} is the PV efficiency.

4. Results and discussion

The lighting condition analysis for the proposed office module in this study was focused on the horizontal surface of a working plan, which was placed anywhere across the room. The working plane was taken as 0.7 m above the floor for offices based upon the definition of BREEAM UK New Construction for Non-domestic Buildings [32]. In addition, energy consumption during a specific time was considered. In this section, the simulation results of indoor lighting conditions and energy performance for the two Models are discussed.

4.1. The effects of BIPV-DSF on indoor lighting conditions

To investigate the overall effect on daylighting incorporating the BIPV-DSF, the simulated illuminance and daylight factor maps showing

the achieved levels in the office module were presented in a 100 × 100 mm grid setting. The following simulations were produced to present the illuminance levels based on the BREEAM assessment criterion – Visual Comfort for Health and Wellbeing [32], which defines suitable daylighting conditions for an office environment described in Table 4.

Fig. 3 represents the daylighting results at the working plane level (0.7 m of height) within Model 1, where a DSF office module with Double Low-E Clear glazing was fitted to the external façade and internal partition. It can be seen from the south facing glazed façade that daylight entered the cavity zone at the highest daylight factor and illuminance levels. Within the occupied zone (including 0.5 m perimeter exclusion zone), the illuminance level adjacent to the internal partition peaked at 909 lux and 9.08% of daylight factor but degraded to 41 lux and 0.42% of daylight factor for the rear of the room. It is noted that both the illuminance levels and DF on the working plane adjacent to the internal partition and central area met the BREEAM pass requirement but, fell below the requirement of average illuminance level (300 lux) and DF (2%) in the rear half of the room.

According to the BREEAM Health and Wellbeing report produced in DesignBuilder (as shown in Table 5), the occupied zone in Model 1 had an acceptable level of daylighting in terms of the average DF and hours at least 300 lux per year, as the simulated results exceeded the corresponding minimum pass requirements by BREEAM. However, it is noted that under these conditions, artificial lighting would be required to increase the illuminance levels towards the rear of the room to meet the minimum DF as per the BREEAM requirement and the recommended illuminance level by the SLL Code for Lighting [29].

The daylight results at the working plane level within the Model 2 are presented in Fig. 4, which was a DSF office module with Amorphous Silicon (a-Si) BIPV glazing fitted to the external façade and Double Low-E Clear glazing fitted within the internal partition. It can be seen from the south-facing glazed façade that daylight entered the cavity zone at the highest daylight factor (6.03%) and illuminance level (603 lux). Looking at the occupied zone in the office module, the daylight levels adjacent to the internal partition (including 0.5 m perimeter exclusion zone) reached the highest values at 243 lux and 2.43% of daylight factor, which had been significantly degrading to 0 lux and 0.00% of daylight factor, respectively, in a rear corner of the room. Comparing with Model 1, the maximum illuminance level in Model 2 dropped by approximately 73%. Consequently, most of the working plane area in Model 2 did not adhere to 300 lux for the proposed office environment according to the SLL Code for Lighting [29].

The BREEAM Health and Wellbeing report produced in DesignBuilder, therefore, indicates this configuration (Model 2) a "failure", as the following results shown in Table 6 for the office module failed to meet all the requirements. Thus, under these conditions, artificial lighting would be required to increase the lighting levels towards the entire room to achieve visual comfort for the room.

In addition, the variations in different lighting parameters between Model 1 and Model 2 can be seen in Fig. 5. Both the calculated average daylight factor and uniformity ratio were seen to decrease by a factor of 73.7% and 50.2% respectively when a-Si PV glazing was introduced (for the Model 2). There are no requirements defining a minimum daylight factor to be achieved, however, both BREEAM [32] and Code of Practice for Daylighting [42] defined an average daylight factor of >2% is to be achieved for a suitably lit environment, which the Model 2 could not achieve. It is also noted that the uniformity ratio for each model presented in Fig. 5 did not meet a minimum of 30% defined in the BREEAM requirements for daylighting conditions in general. Furthermore, the "floor area within limits" refer to the minimum floor area of the office room must have a view of sky from the working plane height, and BREEAM defines this limit of threshold as 80%. Looking at the histogram in Fig. 5, both models were unable to comply with the threshold especially for Model 2, which was far behind the threshold as less than 10% floor area was within the limits. Therefore, both Model 1 and Model 2 require artificial lighting at the north end of the office module to increase the above-mentioned ratios as pure daylighting was calculated to be likely insufficient for an office working environment.

Fig. 6 shows the variations of daylight illuminance on the working plane along the central line from the window to far end in the room. It can be seen that the daylight illuminance was being decreased as the distance to window increasing for both models. However, the illuminance level was maintained properly in Model 1, where the centre of the room also reached the comfortable level around 300 lux. In comparison, the daylight illuminance at the working plane for Model 2 was lower than the recommended 300 lux across the room due to the poor visible light transmittance of the a-Si PV glazing in the BIPV-DSF. This would result in additional artificial lighting required to create reasonable lighting conditions for office environments using BIPV-DSF.

Furthermore, annual daylight calculations including minimum daylight illuminance were also performed in accordance with the BREEAM assessment method to determine if the office modules were sufficiently lit over the course of the year. Table 7 presents the passing BREEAM criteria required to define the occupied zone as suitably lit. It can be seen that both the Model 1 (with Double Low-E Clear glazing) and Model 2 (with a-Si BIPV semi-transparent glazing) did not meet the criteria, but Model 1 nearly reached the requirements of the criteria. As a matter of fact, the introduction of further daylighting measures (for example, glazed roofs such skylights or atria) needs to be considered in a future study to enhance natural light within the space especially for the Model 2 type of rooms.

4.2. The effects of BIPV-DSF on building energy performance

A basic EnergyPlus simulation was performed using DesignBuilder V7 under the Gatwick climate conditions in London of the UK to understand the effects on heating and cooling and lighting capacity due to the installation of the semi-transparent BIPV glazing. Energy modelling required in this research borrowed the principle of the naturally-ventilated BIPV-DSF demonstrated by Yang et al. [26], therefore the ventilation louvres on the external façade drove natural ventilation across the cavity. Specifically, the ventilation louvres were kept being opened and closed to minimise summer cooling and winter heating requirements, respectively. In terms of the simulation period, annual and typical summer (from 17th to 23rd August) and winter (from 1st to 7th December) weeks' building heat balance and PV electrical production were considered.

As shown in Fig. 7, the lighting gain of Model 2 was noticeably higher than Model 1 by 42%, which further proved that the higher artificial lighting demand for the building with BIPV-DSF. It is also seen that there was an inverse relationship between solar gain (through windows) and heating gain, which means the shading effect of the semi-transparent glazing (Model 2) diminished the useful solar heat and thus increased the heating demand. In addition, Model 2 had a lower cooling loss than Model 1 (about 6.5 kWh/m^2 lower), which probably benefitted from the lower solar transmittance of the semi-transparent a-Si PV glazing; and the use of different external window glazing made the indoor pressure

Table 4
Design parameters in daylighting simulation for the BIPV-DSF.

Calculation type	Design parameters
Working plane	0.7 m
Perimeter margin	0.5 m
Sky method	Standard Sky
Sky model	CIE overcast day
Zenith illuminance	10,000 lux
Simulation mode	Annual climate-based daylighting with DAYSIM
Required illuminance level by SLL	300 lux
BREEAM pass requirements	Daylight Factor (DF): average DF > 2%, uniformity ratio >0.3, minimum DF ≥ 0.8% Illuminance level: average 300 lux for 2000 h/year, minimum 90 lux for 2000 h/year

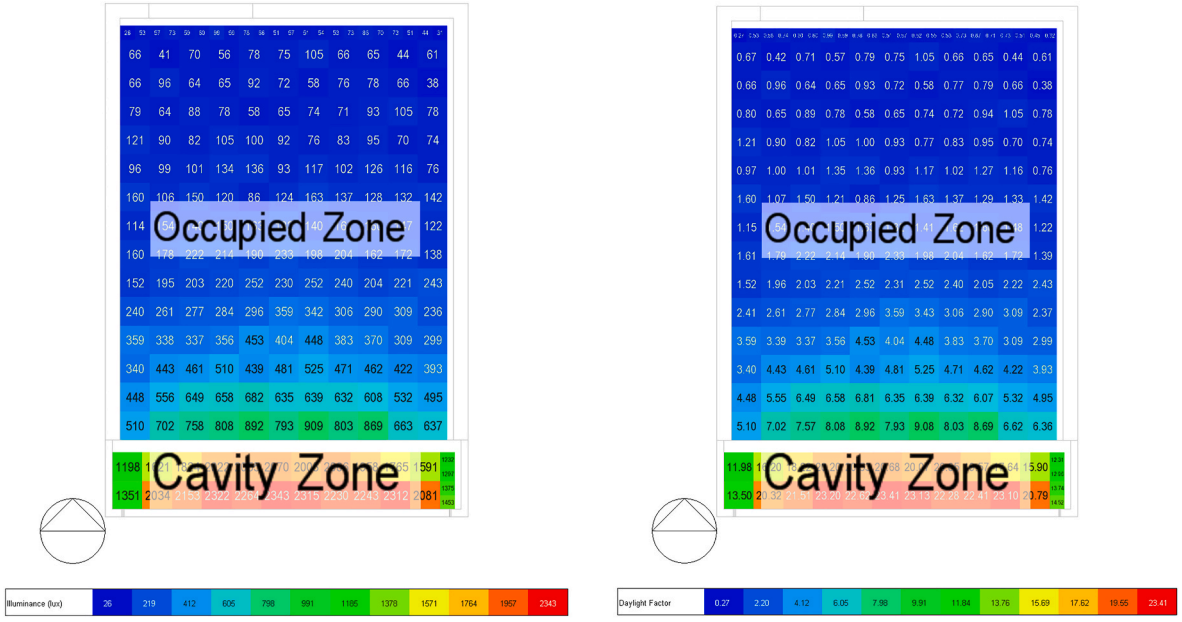

Fig. 3. Daylight distribution in Model 1 – illuminance (left), daylight factor (right).

Table 5
Simulated DF and daylight illuminance hours in comparison with the BREEAM requirements – occupied zone in Model 1.

Parameters to be assessed	Simulated results	BREEAM requirements	Pass/ Fail
Average daylight factor (DF)	2.5%	>2%	Pass
Minimum daylight factor (DF)	0.42%	≥0.8%	Fail
Hours at least 300 lux per year	2626	≥2000 h	Pass

slightly different for such a small office module and consequently led to the different air infiltration between both models. In terms of the use of BIPV, 1.3 kWh/m^2 of PV production in Model 2 was insufficient to compensate the artificial lighting demand due to the considerable low efficiency ($\eta = 3.42\%$) of the semi-transparent a-Si PV glazing used. Note that the 1.3 kWh/m^2 of PV production was per floor area, which was equivalent to only 8.72 kWh generation over a year from three 43 W_p a-Si PV modules. As a matter of fact, the reduced light absorbance

Table 6
Simulated DF and daylight illuminance hours in comparison with the BREEAM requirements – occupied zone in Model 2.

Parameters to be assessed	Simulated results	BREEAM requirements	Pass/ Fail
Average daylight factor (DF)	0.65%	>2%	Fail
Minimum daylight factor (DF)	0.00%	≥0.8%	Fail
Hours at least 300 lux per year	1281 h	≥2000 h	Fail

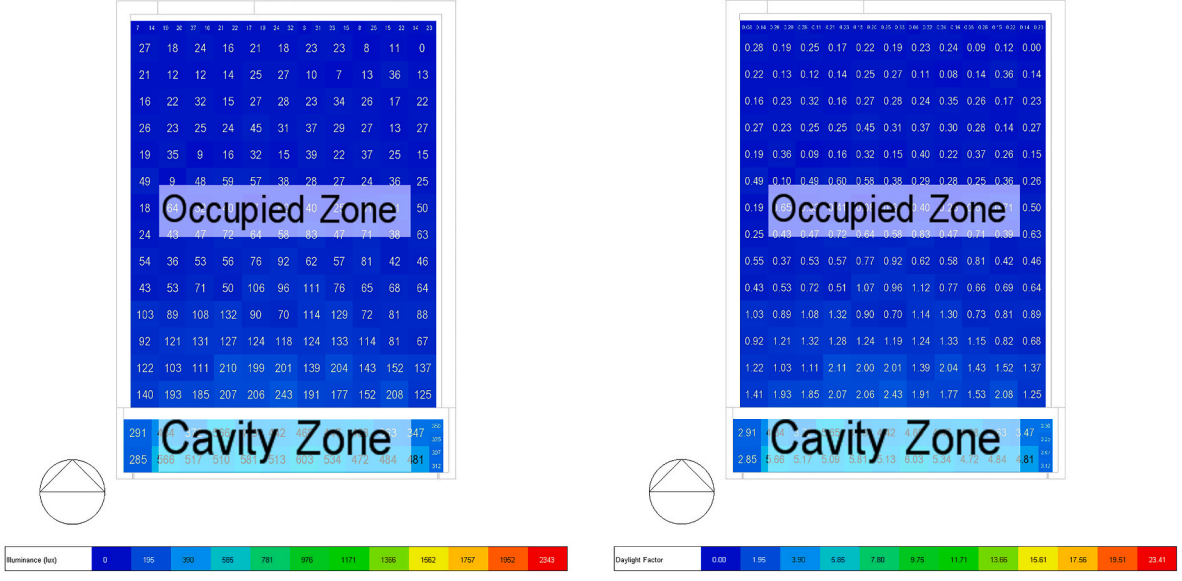

Fig. 4. Daylight distribution in Model 2 – illuminance (left), daylight factor (right).

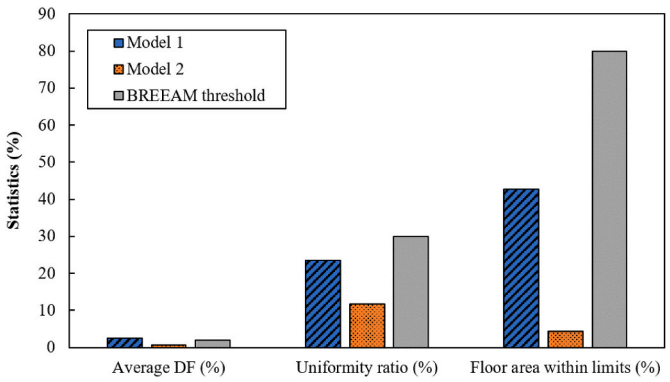

Fig. 5. Cross comparison of the DF, uniformity ratio and floor area within limits between both models and BREEAM requirements.

determines semi-transparent PVs have much lower efficiency than opaque ones [43].

Looking at the design weeks' energy performance (Figs. 8 and 9), the lighting gain of Model 2 was significantly higher than Model 1 by about 64% over the summer design week, which reflects that there was a higher artificial lighting demand for the office module using BIPV-DSF in the summer; Model 2 also had a higher lighting gain compared to Model 1 over the winter design week, but the difference was little (about 26%) due to the inherent lack of sunlight in UK's winter time. Heating gain, which reflects the heating demand, was seen to remain about the same for both models during the summer period, with Model 2 having 0.051 kWh/m^2 of additional heating. During the winter period, Model 2 had a slight increase of 0.696 kWh/m^2 in heating gain due to the reduction of solar gain through the lower solar transmittance PV glazing. However, Model 2 experienced a drop in cooling loss of 0.41 kWh/m^2 in summer in comparison with Model 1, which just benefitted from PV glazing's lower solar transmittance. Moreover, in both summer and winter under London climatic conditions, the a-Si BIPV glazing for Model 2 could not produce sufficient energy to achieve a net zero energy consumption for either season, but a net energy saving about 42% achieved in summer.

Table 8, over the two design weeks, shows a net increase of 0.577 kWh/m^2 (approximately 8%) in energy consumption for Model 2 in comparison with Model 1, which includes the contribution from the BIPV window glazing. It is seen that the total summer energy reduced by 0.228 kWh/m^2 (equivalent to 15%) in Model 2 against Model 1, which was due to the significant cooling demand reduction through the higher shading effect of the semi-transparent BIPV glazing. However, the shading effect of the BIPV glazing led to an overwhelming increase (0.7 kWh/m^2, three times of the reduction in cooling) in heating demand during winter, which consequently caused a disproportionate increase in overall energy consumption for Model 2 with reference to Model 1.

5. Conclusions

This paper assessed both internal lighting conditions and energy performance of a typical office module with double-skin façade (DSF) in London, United Kingdom where semi-transparent BIPV glazing was installed on the external façade for generating renewable energy. The façade is also known as "BIPV-DSF" (Building-Integrated Photovoltaic in Double-Skin Facade). Using the DAYSIM simulation engine in Design-Builder V7 interface, two DSF office models about daylighting simulation were produced, where a reference model (that is, Model 1) presented a DSF installation with both layers of the facade incorporating Double Low-E Clear glazing to represent the visible light transmittance (VLT) values of typical clear glazing. Another model (that is, Model 2, the BIPV-DSF) was produced to represent the BIPV installation on the external layer of the façade, where an Amorphous Silicon (a-Si) PV glazing was selected due to its reasonable efficiency rating, reliability and VLT values amongst different PV options. Based on the BREEAM assessment method for daylighting, it was concluded that the BIPV-DSF had a significant effect on the indoor daylighting conditions, where the maximum illuminance level within the occupied zone dropped by approximately 73% compared to the regular DSF. Furthermore, the average and minimum daylight factors for the BIPV-DSF office module were 0.65% and 0.00% respectively, which did not meet the BREEAM's requirements – not less than 2% and 0.8%, respectively.

The study also found that the building using regular DSF with clear glazing (Model 1) failed to meet the BREEAM assessment criteria by a small margin only, while the building with BIPV-DSF (Model 2) failed significantly against the criteria, and therefore artificial lighting was required to create suitable visual comfort within the building. Further research is required to understand whether additional daylighting provisions such as skylights and light shelves can provide sufficient

Table 7
Annual daylight illuminance hours against the BREEAM requirements – both models.

Criteria	Model 1	Model 2	BREEAM requirements
Minimum daylight illuminance (hours at least 90 lux per annum)	1814	229	≥2000 h/year
Average daylight illuminance (hours at least 300 lux per annum)	2626	1281	≥2000 h/year
Pass/Fail	Fail	Fail	

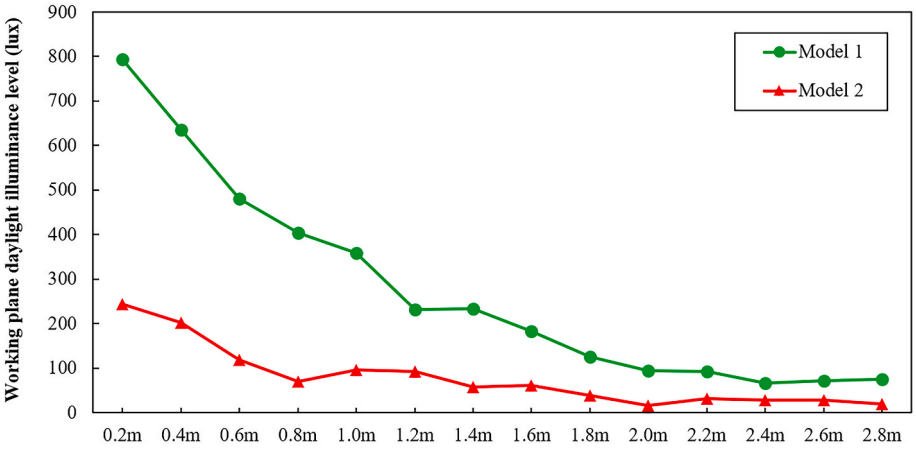

Fig. 6. Daylight illuminance on the working plane along the central line from window to far end.

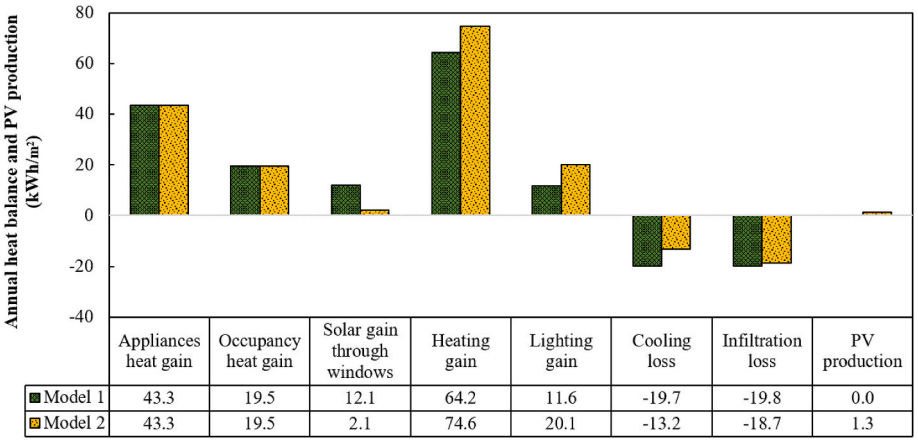

	Appliances heat gain	Occupancy heat gain	Solar gain through windows	Heating gain	Lighting gain	Cooling loss	Infiltration loss	PV production
Model 1	43.3	19.5	12.1	64.2	11.6	-19.7	-19.8	0.0
Model 2	43.3	19.5	2.1	74.6	20.1	-13.2	-18.7	1.3

Fig. 7. Annual building heat balance and PV production for both models.

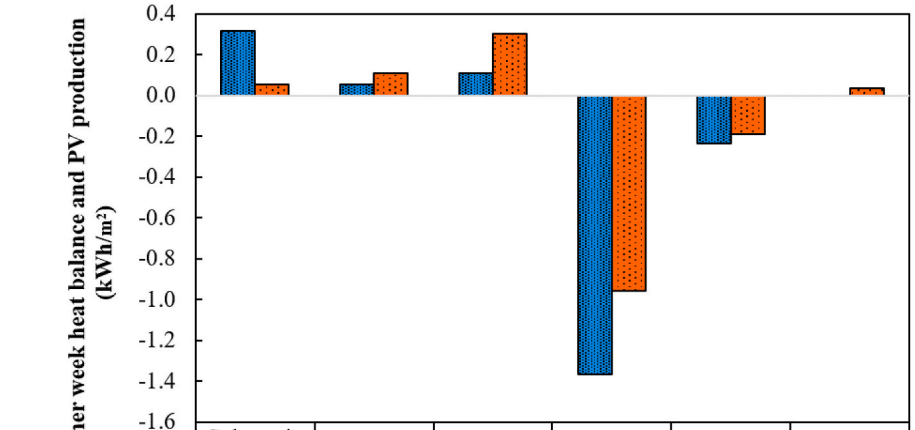

	Solar gain through windows	Heating gain	Lighting gain	Cooling loss	Infiltration loss	PV production
Model 1 Summer	0.314	0.056	0.110	-1.368	-0.236	0.000
Model 2 Summer	0.053	0.107	0.302	-0.958	-0.187	0.035

Fig. 8. Building heat balance and PV production for both models in a typical summer week.

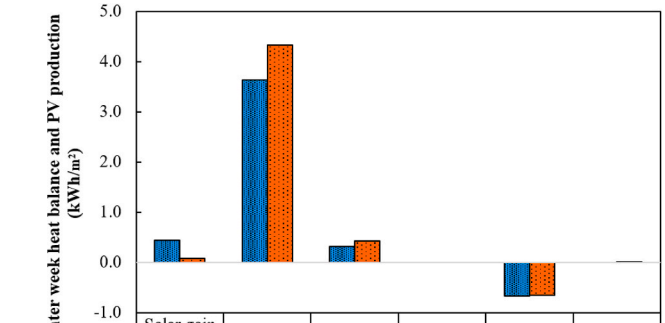

	Solar gain through windows	Heating gain	Lighting gain	Cooling loss	Infiltration loss	PV production
Model 1 Winter	0.441	3.634	0.313	0.000	-0.668	0.000
Model 2 Winter	0.076	4.330	0.425	0.000	-0.664	0.006

Fig. 9. Building heat balance and PV production for both models in a typical winter week.

daylighting rectification to mitigate the impact of the reduced daylight intensity due to the configuration of BIPV-DSF for the building, which is also related to the control of artificial lighting for the environmental conservation.

Table 8
Net energy consumptions for both models over the typical design weeks.

Category	Model 1		Model 2	
	Summer	Winter	Summer	Winter
Lighting (kWh/m^2)	0.110	0.313	0.302	0.425
Heating (kWh/m^2)	0.060	4.769	0.113	5.468
Cooling (kWh/m^2)	1.354	–	0.916	–
PV production (kWh/m^2)	–	–	0.035	0.006
Subtotal of energy consumption (kWh/m^2)	1.524	5.082	1.296	5.887
Total energy consumption (kWh/m^2)	6.606		7.183	

In terms of energy performance, various studies have demonstrated that the BIPV-DSF is able to maintain a reasonable indoor thermal condition as well as reduce the overall energy uses for buildings in temperate climates. In addition to the major concern of indoor visual comfort, the study presented in this paper, using the EnergyPlus simulation engine embedded in DesignBuilder programme, assessed energy performance of the proposed office module with BIPV-DSF in the cold climate zone (that is, London, UK). It was found that this configuration of BIPV-DSF was not able to produce sufficient electrical energy to make

up for the increase in artificial lighting and the increased heating capacity in winter under London's climatic conditions due to the low visible light transmittance and low efficiency ($\eta = 3.42\%$) of the semi-transparent glazing window used. However, it should be noted that a net reduction of 15% in energy was recorded in the summer months due to both electrical production and shading effects from the BIPV-DSF.

Given that the cold seasons usually run longer in the UK than that of Southern European countries, heating energy consumption should be the predominant factor other than lighting energy when appraising the performance of the BIPV-DSF. Therefore, it is concluded that the uptake of this BIPV-DSF configuration is not recommended under the UK's climate conditions or equivalents in the present context. As not only the comfortable indoor lighting condition is barely maintained, but also the energy production of the BIPV-DSF is insufficient to overcome the net heating load over the cold seasons at present. In order to extend the applicability of such a novel façade technology in various climate zones, further research needs to be focused on the improvement of power conversion efficiency and visible light transmission for the semi-transparent PV glazing.

CRediT authorship contribution statement

Frank Roberts: Data curation, Formal analysis, Writing – original draft. **Siliang Yang:** Conceptualization, Methodology, Supervision, Software, Validation, Visualization, Investigation, Formal analysis, Writing – review & editing. **Hu Du:** Software, Validation, Visualization, Investigation, Formal analysis, Writing – review & editing. **Rebecca Yang:** Writing – review & editing.

Declaration of competing interest

The authors declare that they have no known competing financial interests or personal relationships that could have appeared to influence the work reported in this paper.

Data availability

Data will be made available on request.

Acknowledgements

This study received the support from the European Commission's Horizon 2020 research and innovation programme under the grant agreement No. 768735.

References

[1] H.J. Han, et al., New developments in illumination, heating and cooling technologies for energy-efficient buildings, Energy 35 (6) (2010) 2647–2653.
[2] United Nations Environment Programme, 2021 Global Status Report for Buildings and Construction: towards a Zero-Emission, Efficient and Resilient Buildings and Construction Sector, 2021 (Nairobi).
[3] R.T. Hellwig, et al., Design of adaptive opportunities for people in buildings, in: Routledge Handbook of Resilient Thermal Comfort, Routledge, 2022, pp. 193–209.
[4] M. Conci, et al., Trade-off between the economic and environmental impact of different decarbonisation strategies for residential buildings, Build. Environ. 155 (2019) 137–144.
[5] Y. Wang, et al., A review of approaches to low-carbon transition of high-rise residential buildings in China, Renew. Sustain. Energy Rev. (2020) 131.
[6] H. Du, P. Huang, P. Jones, Modular facade retrofit with renewable energy technologies: the definition and current status in Europe, Energy Build. (2019) 205.
[7] S. Yang, et al., Numerical simulation modelling of building-integrated photovoltaic double-skin facades, in: F. Bulnes, J.P. Hessling (Eds.), Recent Advances in Numerical Simulations, IntechOpen, London, United Kingdom, 2021, pp. 61–75.
[8] R.A. Agathokleous, S.A. Kalogirou, Double skin facades (DSF) and building integrated photovoltaics (BIPV): a review of configurations and heat transfer characteristics, Renew. Energy 89 (2016) 743–756.
[9] N. Martín-Chivelet, et al., Building-integrated photovoltaic (BIPV) products and systems: a review of energy-related behavior, Energy Build. (2022) 262.
[10] S. Habibi, O.P. Valladares, D.M. Peña, Sustainability performance by ten representative intelligent façade technologies: a systematic review, Sustain. Energy Technol. Assess. (2022) 52.
[11] S. Yang, et al., Study of building integrated photovoltaic/thermal double-skin facade for commercial buildings in Sydney, Australia, in: Final Conference of COST TU1403 "Adaptive Facades Network", Lucerne, Switzerland, 2018.
[12] S. Attia, et al., Comparison of thermal energy saving potential and overheating risk of four adaptive façade technologies in office buildings, Sustainability 14 (10) (2022).
[13] F. Ascione, et al., The evolution of building energy retrofit via double-skin and responsive façades: a review, Sol. Energy 224 (2021) 703–717.
[14] P.C. Wong, D. Prasad, M. Behnia, A new type of double-skin façade configuration for the hot and humid climate, Energy Build. 40 (10) (2008) 1941–1945.
[15] N. Hashemi, R. Fayaz, M. Sarshar, Thermal behaviour of a ventilated double skin facade in hot arid climate, Energy Build. 42 (10) (2010) 1823–1832.
[16] Z.S. Zomorodian, M. Tahsildoost, Energy and carbon analysis of double skin façades in the hot and dry climate, J. Clean. Prod. 197 (2018) 85–96.
[17] Y. Wang, Y. Chen, J. Zhou, Dynamic modeling of the ventilated double skin façade in hot summer and cold winter zone in China, Build. Environ. 106 (2016) 365–377.
[18] A.L.S. Chan, et al., Investigation on energy performance of double skin façade in Hong Kong, Energy Build. 41 (11) (2009) 1135–1142.
[19] J. Zhu, G. He, Heat transfer coefficients of double skin facade windows, Sci. Technol. Built Environ. 25 (9) (2019) 1143–1151.
[20] J. Han, et al., Performance of ventilated double-sided PV façade compared with conventional clear glass façade, Energy Build. 56 (2013) 204–209.
[21] J. Peng, L. Lu, H. Yang, An experimental study of the thermal performance of a novel photovoltaic double-skin facade in Hong Kong, Sol. Energy 97 (2013) 293–304.
[22] J. Peng, et al., Numerical investigation of the energy saving potential of a semi-transparent photovoltaic double-skin facade in a cool-summer Mediterranean climate, Appl. Energy 165 (2016) 345–356.
[23] C. Qiu, H. Yang, Daylighting and overall energy performance of a novel semi-transparent photovoltaic vacuum glazing in different climate zones, Appl. Energy (2020) 276.
[24] S. Yang, et al., Studies on optimal application of building-integrated photovoltaic/thermal facade for commercial buildings in Australia, in: Proceedings of SWC2017/SHC2017, 2017, pp. 1–10.
[25] S. Yang, et al., Numerical simulation study of BIPV/T double-skin facade for various climate zones in Australia: effects on indoor thermal comfort, Build. Simulat. 12 (1) (2018) 51–67.
[26] S. Yang, et al., Performance assessment of BIPV/T double-skin façade for various climate zones in Australia: effects on energy consumption, Sol. Energy 199 (2020) 377–399.
[27] S. Yang, et al., A sensitivity analysis of design parameters of BIPV/T-DSF in relation to building energy and thermal comfort performances, J. Build. Eng. (2021) 41.
[28] C. Giarma, K. Tsikaloudaki, D. Aravantinos, Daylighting and visual comfort in buildings' environmental performance assessment tools: a critical review, Procedia Environ. Sci. 38 (2017) 522–529.
[29] The Society of Light and Lighting, The SLL Code for Lighting, 2012.
[30] The building Regulations, approved document L2A, in: Conservation of Fuel and Power in New Buildings other than Dwellings, HM Government, 2010.
[31] A. Ghosh, S. Sundaram, T.K. Mallick, Investigation of thermal and electrical performances of a combined semi-transparent PV-vacuum glazing, Appl. Energy 228 (2018) 1591–1600.
[32] Building Research Establishment, *BREEAM UK New Construction* in *Non-domestic Buildings Technical Manual*, 2018.
[33] N. Ziasistani, F. Fazelpour, Comparative study of DSF, PV-DSF and PV-DSF/PCM building energy performance considering multiple parameters, Sol. Energy 187 (2019) 115–128.
[34] M. Shakouri, H. Ghadamian, A. Noorpoor, Quasi-dynamic energy performance analysis of building integrated photovoltaic thermal double skin façade for middle eastern climate case, Appl. Therm. Eng. (2020) 179.
[35] F. Fazelpour, et al., An assessment of reducing energy consumption for optimizing building design in various climatic conditions, Int. J. Energy Environ. Eng. 13 (2022) 319–329.
[36] G.J. Ward, The RADIANCE lighting simulation and rendering system, in: Proceedings of the 21st Annual Conference on Computer Graphics and Interactive Techniques, 1994.
[37] C.F. Reinhart, O. Walkenhorst, Validation of dynamic RADIANCE-based daylight simulations for a test office with external blinds, Energy Build. 33 (7) (2001) 683–697.
[38] C. Reinhart, P.-F. Breton, Experimental validation of Autodesk® 3ds Max® design 2009 and daysim 3.0, Leukos 6 (1) (2013) 7–35.
[39] G. Yun, K.S. Kim, An empirical validation of lighting energy consumption using the integrated simulation method, Energy Build. 57 (2013) 144–154.
[40] R. Perez, R. Seals, J. Michalsky, All-weather model for sky luminance distribution—preliminary configuration and validation, Sol. Energy 50 (3) (1993) 235–245.
[41] R.D. Taylor, C.O. Pedersen, L. Lawrie, Simultaneous simulation of buildings and mechanical systems in heat balance based energy analysis programs, in: Proceedings of the 3rd International Conference on System Simulation in Buildings, Citeseer, 1990.
[42] British Standards Institution, BS 8206-2, in: Lighting for Buildings - Part 2: Code of Practice for Daylighting, 2018.
[43] S. Lie, et al., Semitransparent perovskite solar Cells with > 13% Efficiency and 27% transperancy using plasmonic Au nanorods, ACS Appl. Mater. Interfaces 14 (9) (2022) 11339–11349.